SHORT COMMUNICATION

Synthesis of Cobalt Oxide Nanoparticles/Fibres in Alcoholic Medium using γ-ray Technique

Anjali A. Athawale[*], Megha Majumdar, Hema Singh, and K.Navinkiran

University of Pune, Pune-411 007
[*]*E-mail: agbed@chem.unipune.ernet.in*

ABSTRACT

Nanoparticles of cobalt oxides were synthesised by steady state γ irradiation technique using various alcoholic salt solutions of cobalt ions with aniline acting as a stabiliser. Preliminary results were investigated using UV-vis and Fourier transform infra red analysis. The X-ray diffractograms revealed major peaks at 2θ values of ~ 36.4°, 39.1°, 44.2°, and 65.7° corresponding to the Co_3O_4 phase and one peak at ~30.7° (100 per cent intensity) for Co_2O_3 phase. Lower alcohols yielded particles while fibres were formed in higher alcohols as observed from transmission electron microscopic analysis. Iso-propanol was observed to yield cobalt oxide nanoparticles with highest stability, conversion yield and homogeneity in size. The average measured diameter and length of these fibres were ~29 nm and 130 nm respectively. Energy dispersive spectroscopy supports the formation of cobalt oxide. The X-ray photoelectron spectroscopic results for iso-propanol sample show a peak at 781.6 eV confirming the formation of Co_3O_4.

Keywords: Oxides, X-ray diffraction, X-ray photoelectron spectroscopy, XPS, optical properties, γ irradiation technique, magnetic nanoparticles, UV-visible spectroscopy, spectroscopy, cobalt-oxide nanoparticles, nanoparticle synthesis

1. INTRODUCTION

Magnetic nanoparticles have important applications in catalysis[1], ferrofluids[2], high-density recording media[3], microwave absorbing materials[4], etc. The preparation of nanoscale magnetic materials with desired properties is difficult, especially magnetic transition metal oxide nanoparticles like nickel, cobalt and iron, present a significant challenge. Cobalt oxide-based materials have been widely used for energy storage systems, electrochromic thin films, magnetoresistive devices, and heterogeneous catalysis. In the presence of CO and H_2, thin films of Co_3O_4 show reversible changes in the Vis-near IR absorption band[5]. This phenomenon can be applied in the fabrication of solid-state gas sensors. Thin films of lithium-doped Co_3O_4 have been reported to exhibit change in colour from brown-to-light yellow[6]. The reversible changes in optical properties of Co_3O_4 under an external stimulus can be used to fabricate electrochromic devices[7]. Such a broad perspective of utilisation has increased the importance of synthesising cobalt oxide nanoparticles.

Metal oxide nanocrystals have also been utilised for the destructive adsorption of warfare agents. The nanoparticles, which can be used on both acids and bases, bind to molecules of the hazardous substances and convert these to safer by-products rapidly. The use of magnetic nanoparticles to detoxify contaminated military personnel or civilians following a poison gas attack is under investigation by several research groups. Areas currently under investigation include nanoparticles to make smart coating on vehicles, nanosensors in light weight uniforms, sensors to detect life signs, and advanced computing power for code breaking and encryption.

Various methods such as spray pyrolysis[8], plasma sputtering[9], thermal salt decomposition[10], powder immobilisation[11], γ-irradiation[12], hydrothermal[13], micro-emulsion[14] sol-gel technique[15] and laser ablation technique[16] have been used so far for the synthesis of metal oxide nanoparticles. Often, synthesis is carried out using water as a solvent[17,18] except few reports quoting non-aqueous solvents.

In the present study, the preparation of nanoparticles/nanofibres of cobalt oxides in alcoholic medium in the presence of aniline as a stabiliser by γ-radiolysis technique is reported. These sols were characterised using UV-visible spectroscopy (UV-vis), Fourier transform infra-red spectroscopy (FT-IR), X-ray diffraction measurements (XRDs) Transmission electron microscopy (TEM) and X-ray photoelectron spectroscopy (XPS). These sols have been tested for catalysis applications.

2. EXPERIMENTAL STUDIES
2.1 Materials Used

All the reagents used were of AR grade with 99.5 per cent purity. Cobalt nitrate ($Co(NO_3)_2, 6H_2O$) cobalt chloride ($CoCl_2, 6H_2O$) and cobalt acetate ($Co(Ac)_2, H_2O$) were procured from Loba Chemie. The alcohols (methanol, ethanol, *n-*

propanol, iso-propanol, *n*-butanol and *n*-hexanol), aniline ($C_6H_5NH_2$) and ammonium persulphate (($NH_4)_2S_2O_8$) were obtained from Qualigens, India. All the alcohols and aniline were distilled before use, aniline was stored in dark under refrigeration. Millipore water was used throughout the experiment. Stock solutions of 0.1M concentration of cobalt salts were prepared in water and used for the experiments.

2.2 Methods of Preparation and Characterisation Techniques

For preparing nanoparticles, cobalt salts such as nitrates, chlorides, and acetates were used and conversions were observed only in presence of nitrate salts. Hence, further experiments were pursued using cobalt nitrate solution. Concentration of cobalt ions were varied from 1×10^{-3} – 1×10^{-2} M and that of aniline from $0.1 - 0.01$ M. Results were best at concentration of cobalt ions and aniline as 3×10^{-3} and 0.1 M, respectively. The solutions containing cobalt ions and aniline in different alcohols such as methanol, ethanol, n-propanol, iso-propanol (IPA), *n*-butanol, and *n*-hexanol were irradiated in a ^{60}Co γ-ray source for different time intervals (up to 72 h) at a dose rate of 5.1 Gy min^{-1}.

After obtaining the nanosols, these were characterised using various techniques such as UV-visible (UV-vis) spectroscopy and fourier transform infra red spectroscopy (FT-IR), X-ray diffraction measurements (XRD), transmission electron microscopy (TEM), energy dispersive spectroscopy (EDS) and X-ray photoelectron spectroscopy (XPS). Composites (Pani-Cobalt oxide prepared by polymerising the sol) were used for FT-IR and X-ray diffraction analysis.

Absorption spectra of all the samples were recorded on a Shimadzu (1650 PC) spectrophotometer. Spectra were taken at regular intervals with reference to a blank solution without metal ion under identical conditions using double beam spectrophotometer having a path length of 1.00 cm, operated at a resolution of 1 nm from wavelength 350 nm to 900 nm.

FT-IR analysis of samples was done on a Shimadzu 8400 spectrophotometer at a range of 4000–350 cm^{-1}. For this, 10 mg of the dried composite sample was mixed with 100 mg of spectroscopic grade potassium bromide (*KB*r) and the resultant mixture was ground in a mortar and pestle. The sample was pressed into a transparent homogeneous pellet by applying a pressure of 7 tons. Typically, 30 scans per spectrum were recorded at 4 cm^{-1} resolution in the transmittance mode. The background spectrum was automatically subtracted.

Philips X'Pert Pro XRD machine was used with *Ni* filter and *CuK*α source operating at 40 kV and 20 mA to perform crystallographic studies of the prepared nanocomposite powders by rotating anode XRD. Interplanar distances (*d* values) were calculated according to Bragg's law and were compared with the ASTM data to determine the crystal structure. The glancing angle varied from 5° to 80°

TEM micrographs were obtained on a Philips CM 200 microscope using an accelerating voltage of 200 kV. 2 μl

sol was loaded on a carbon-coated copper grid, excessive solution was drained on a filter paper and the solvent was evaporated in air. The point-to-point resolution of the equipment was 0.23 nm. Elemental composition was determined by using EDAX attached to the instrument.

XPS measurements were done using VG Scientific ESCA-3000 spectrometer equipped with a hemispherical analyser and an *Al* anode using *MgK*α (1253.6 eV) operating at a voltage of 12–14 kV and current of 10–20 mA. Samples were mounted onto a conductive adhesive *Cu* tape. Spectra were obtained at room temperature and the operating pressure in the analysis chamber at vacuum was approx 1×10^{-8} Torr. Calibration was performed for carbon correction. The core-level spectra were corrected for background using the Shirley algorithm, and the chemically distinct species were resolved by a nonlinear least square procedure.

3. RESULTS AND DISCUSSION
3.1 UV-Visible Spectroscopy

Nanoparticles of cobalt oxide were obtained by g irradiation of alcoholic solutions of cobalt ions in the presence of aniline. Absence of aniline in the solution during irradiation did not give such a conversion. Figure 1 depicts the time-evolved spectra of the cobalt nanosols in various alcohols (methanol, ethanol, *n*- and iso-propanol, *n*-butanol and *n*-hexanol) after gamma irradiation. Curves (a) in the figure represent the absorbance of unirradiated solutions showing negligible absorbance. The absorbance was seen to increase with irradiation time and a sharp peak was observed in the range of 430-500 nm Curves (b)-(d) in each case can be attributed to the formation of cobalt oxide[19] surrounded with aniline molecules which stabilise the nanoparticles[20].
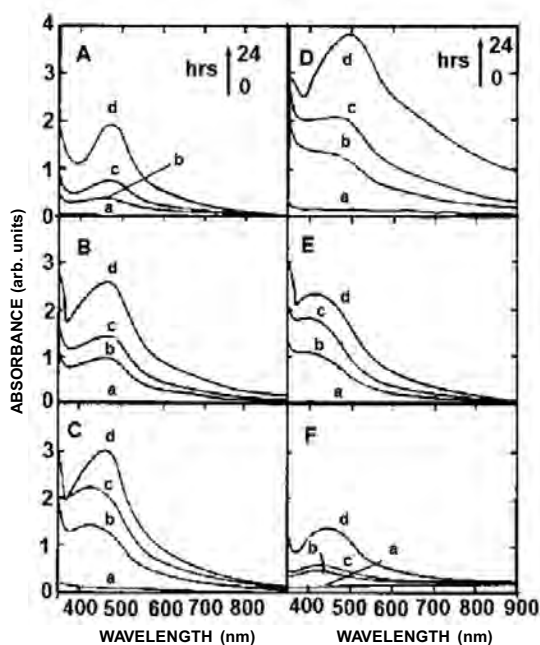

Figure 1. UV-vis spectra of cobalt nanosols obtained after: (a) 0, (b) 4, (c) 7 and (d) 24 h of irradiation in (A) methanol, (B) ethanol, (C) *n*-propanol, (D) iso-propanol, (E) *n*-butanol, and (F) *n*-hexanol.

Transient spectra of aminyl and amine radical cation have also been reported in the region between 415-430 nm [21]. Thus, these absorptions may have an origin in the formation of similar species in the solution.

A comparison of the absorption spectra reveals highest absorbance for iso-propanol indicating maximum conversion of cobalt ions into cobalt oxides. Also, these sols were observed to be stable up to 5-7 days. On the other hand, precipitation was observed in remaining alcohols after 48 h. The stability in the case of iso-propanol can be attributed to its symmetrical structure and polarity facilitating the formation of the product as well as stabilising the particles through weak surface (Vander waal's forces) interactions. In n-hexanol this effect is further enhanced.

In lower alcohols the stabilisation as well as formation is affected due to their small size and higher dielectric constant i.e. polarity.

3.2 FT-IR Spectroscopy

Figure 2 shows the FT-IR spectra of cobalt oxides obtained for selected alcohols. The band at 470 cm^{-1} corresponds to the metal-oxygen (*Co-O*) bond. Additionally, two more distinct peaks at ~687 cm^{-1} and 715 cm^{-1} are indicative of the presence of optical vibration modes of cobalt oxide[19].

3.3 X-ray Diffraction Analysis

Further, the formation of oxide could be confirmed from the X-ray diffraction analysis of the samples. The X-ray diffractograms were scanned between 2θ angles of 5-80°. Figure 3 indicates the X-ray diffractograms of the cobalt oxide nanoparticles obtained in methanol, ethanol, IPA and *n*-butanol. Each diffractogram show the peaks characteristic for the Co_3O_4 phase[22] of cobalt oxide at 2θ values of ~ 36.4°, 39.1°, 44.2° and 65.7° with the corresponding hkl planes of (311), (222), (400) and (440), respectively along with the most intense (100 per cent) peak for Co_2O_3 at ~30.7° (002). These values are in agreement with the data in the JCPDS card no. 42-1467 and 02-0770, respectively.
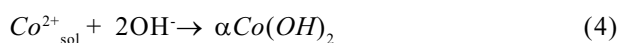
The mechanism of formation probably proceeds through the following reactions. The alcohol undergoes radiolysis giving solvated electrons, hydroxide, isopropyl, and acetonyl radicals along with other radiolysis products
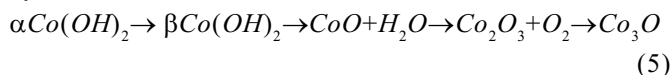
$$R OH \longrightarrow e^-_{sol}, H_{sol}, OH^-, ROH_2^+, RCOH, \text{etc.} \quad (1)$$
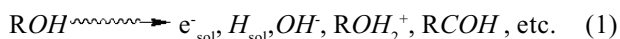
The cobalt ions (Co^{2+}) react with the solvated electrons and undergo reduction to generate Co^+ species. However, the Co^+ ions are highly unstable, hence undergo disproportionation reaction as

$$Co^{2+} + e^-_{sol} \rightarrow Co^+ \quad (2)$$

$$Co^+ + Co^+ \rightarrow Co^0 + Co^{2+} \quad (3)$$
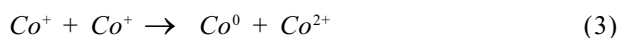
The Co^{2+} ions react with hydroxyl ions forming cobalt hydroxide, a blue coloured suspension (intermediate) which is the α phase cobalt hydroxide.

$$Co^{2+}_{sol} + 2OH^- \rightarrow \alpha Co(OH)_2 \quad (4)$$

The α form is unstable and rapidly changes to β cobalt hydroxide[23].

$$\alpha Co(OH)_2 \rightarrow \beta Co(OH)_2 \rightarrow CoO + H_2O \rightarrow Co_2O_3 + O_2 \rightarrow Co_3O$$

$$(5)$$

The hydroxide finally converts to oxide phase, i.e., *CoO* which subsequently reacts with the oxygen yielding stable phases of Co_2O_3 and Co_3O_4 oxides.
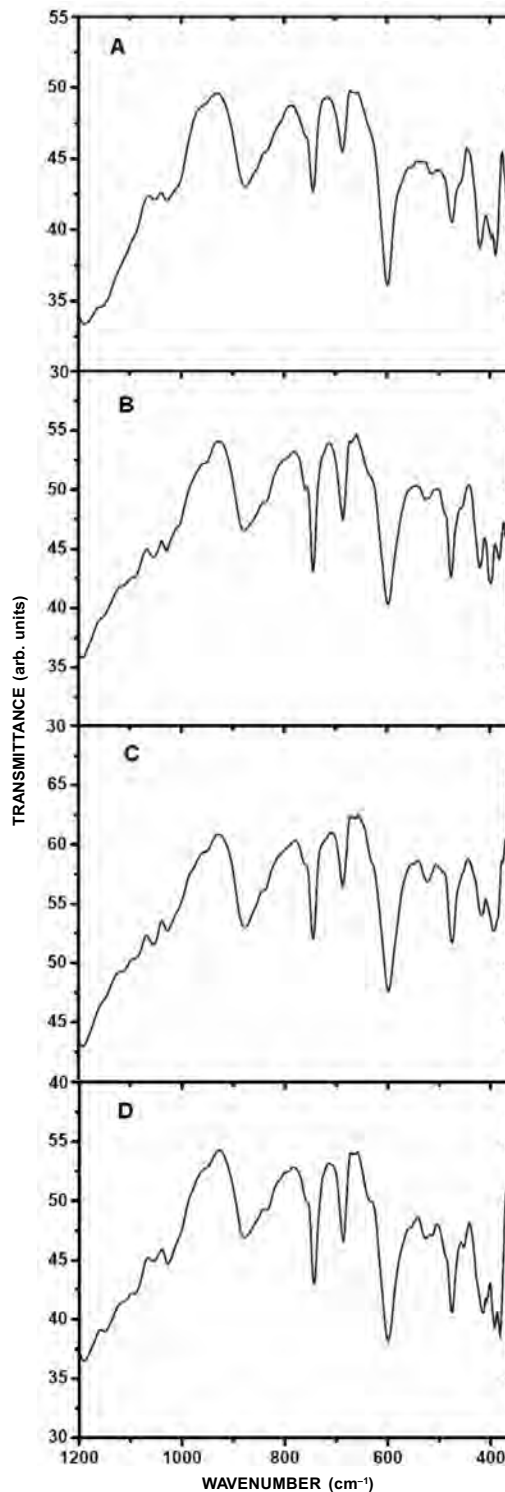

Figure 2. FT-IR spectra of cobalt oxides nanosols: (a) methanol, (b) ethanol (c) iso-propanol, and (d) *n*-butanol.
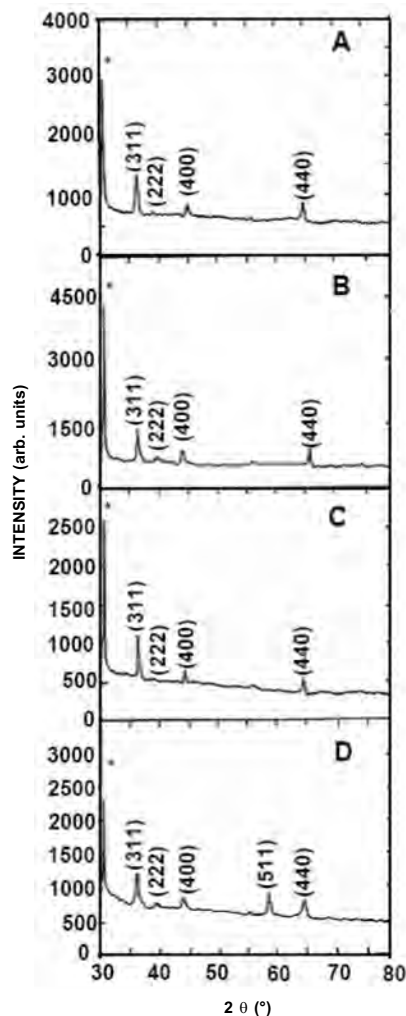
Figure 3. X-ray diffractograms of cobalt oxides: (A) methanol, (B) ethanol, (C) iso-propanol, and (D) *n*-butanol (* represents (002) plane for *Co₂O₃*).

Figure 4. Transmission electron micrographs of cobalt oxide nanosols prepared in: (a) methanol, (b) ethanol, (c) iso-propanol, and (d) *n*-hexanol.

3.4 Transmission Electron Microscopy

TEM micrographs in Fig. 4 are indicative of morphology of the cobalt oxide nanoparticles formed in methanol, ethanol, iso-propanol, and *n*-hexanol. In case of methanol, relatively large-sized particles with an irregular shape are observed with an average size of > 300 nm (Fig. 4 (a)). In ethanol (Fig. 4(b)) more or less spherical particles with an average size of ~90 nm can be noted. However, in higher alcohols, the product exhibits fibrous morphology. In IPA, the fibres appear to be small, thin, and uniformly dispersed throughout the image (Fig. 4(c)) with an average length of ~130 nm and diameter of ~29 nm. Similarly, in *n*-hexanol the fibres seem to have average dimensions of ~200 nm × 26 nm and are agglomerated into a star shape as shown in Fig. 4(d).

In the case of lower alcohols, particle formation is predominant since they have high polarity, and also they are volatile. However, due to their small size agglomeration is stronger.

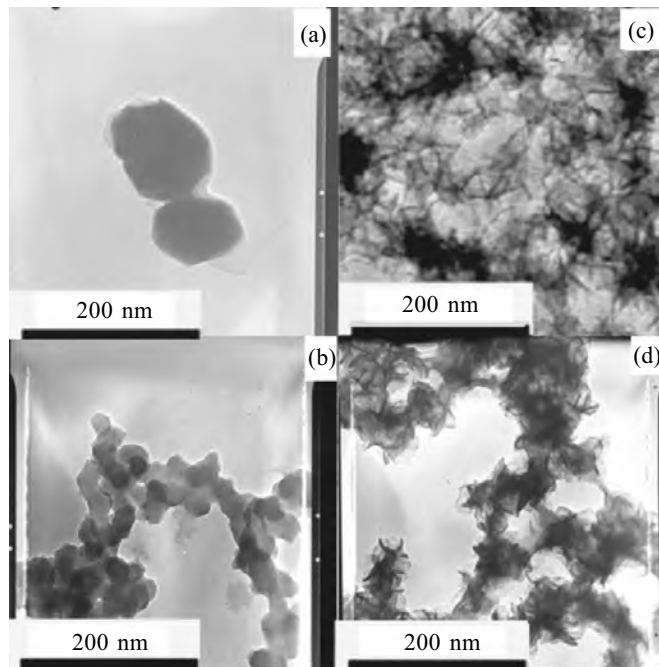On the other hand, iso-propanol and *n*-hexanol are relatively bulkier and have low polarity, therefore, they interact weakly with the nuclei of products (cobalt oxide) formed and at latter time intervals, growth along a particular plane is favoured resulting in fibre formation.

Additionally, SAED and EDS analyses for cobalt oxide sample in IPA support the formation of cobalt oxide. The atomic composition and crystalline nature of the nanoparticles were verified with the help of selected area electron diffraction (SAED) patterns of the cobalt oxide nanosol prepared in IPA, as shown in Fig. 5(a). SAED profiles were first calibrated using 'd' spacing of a single crystalline Au thin film. Some broad as well as diffused rings were observed in the deposited sample. The SAED pattern of the sample shows crystalline nature. The lattice constants obtained for diffraction lines are 0.26 nm and 0.38 nm that can be referred to cobalt oxide phase. Comparison of *d*-spacing with the JCPDS data confirms the formation of Co_3O_4 as the major fraction together with Co_2O_3.

The length and diameter distribution of cobalt oxides fibres (Fig. 4(c)) are shown in Fig. 5(b). The degree of dispersity in diameter is lower as compared to length. The distribution in length is from 77 nm to 217 nm and diameter from 25 nm to 34 nm. The elemental composition and possible molecular formula could be evaluated from the EDS. Spectrum in Fig. 5(c) shows the presence of cobalt, oxygen, carbon, and copper. *Cu* is from copper grid and carbon is in part from carbon film on the surface of the copper grid and partially from the polymer carbonisation[24],[25]. It is evident that presence of both cobalt and oxygen implies the formation of oxide in the synthesised samples. The elemental composition of the fibres shows 33 per cent Co and 66 per cent oxygen in atomic percentage corresponding to cobalt oxide shown in Table 1. The compositional data from the EDS system
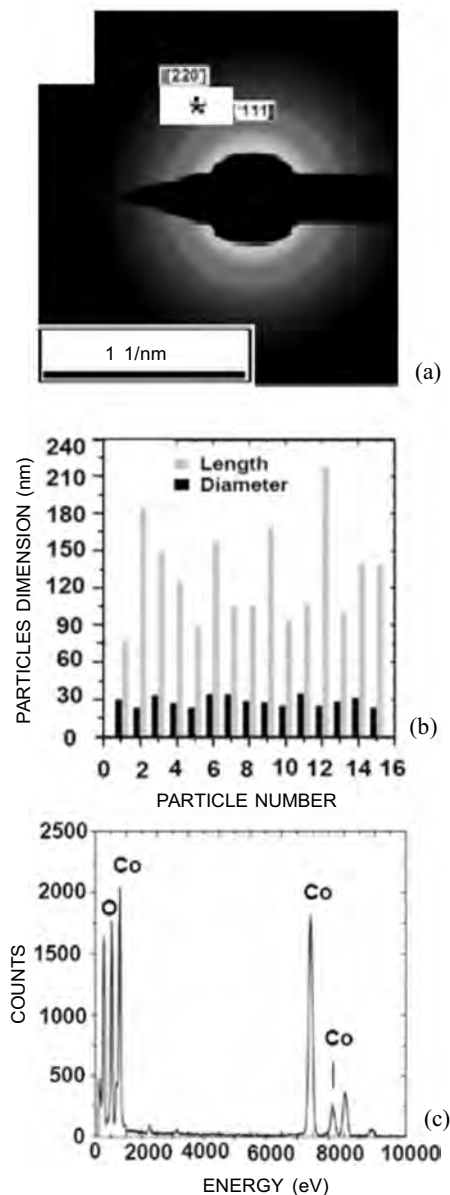
(a)

(b)

(c)

Figure 5. **(a) SAED profile (*) denotes Co_2O_3 phase and the remaining phases are of Co_3O_4 (b) Histogram of length and diameter distributions, and (c) EDAX of cobalt oxide nanosol in iso-propanol.**

agree well with each other and the values match with theoretically calculated values, indicating a good compositional homogeneity across the nanoparticles.

3.5 X-ray Photoelectron Spectroscopy

The surface of the as-prepared nanosol was investigated by XPS, as shown in Fig. 6. In the literature[26], the various

Table 1. EDS data of cobalt oxide nanofibres

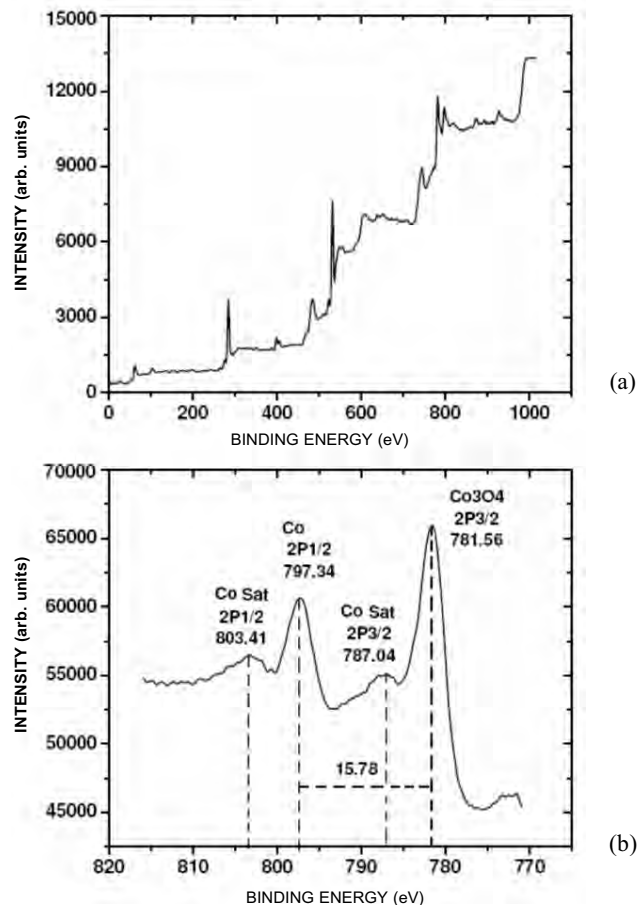| Element	Weight percentage	Atomic percentage	Uncertainity percentage	Detector correction	*k*-factor
O(k)	34.940	66.423	0.357	0.514	1.980
Co(k)	65.059	33.576	0.374	0.995	1.576

(a)

(b)

Figure 6. XPS of cobalt oxide nanosol in iso-propanol: (a) general, and (b) cobalt scan.

oxidation peaks of cobalt are reported at 778.3 eV and 793.3 eV for Co^0, 780.4 eV, 795.8 eV for Co^{2+} and 778.5 eV and 794.2 eV for Co^{3+}.

In the present spectra, the nanosol exhibits Co $2p_{3/2}$ core level peak at a binding energy of 781.6 eV, and Co $2p_{1/2}$ at 797.2 eV with a difference of 15.61 eV which can be attributed to the presence of both Co^{2+}/Co^{3+} species[27].

4. CONCLUSIONS

Cobalt oxide nanoparticles are formed in pure alcohols on gamma radiolysis. Lower alcohols yield spherical particles, while fibres are formed in higher alcohols. As the product obtained has better yield and stability, IPA is found to be the best solvent giving stable and homogeneous nanofibres.

REFERENCES

1. Rodrigues, E.L. & Bueno, J.M.C. Co/SiO_2 catalysts for selective hydrogenation of crotonaldehyde. Part II: Influence of the Co surface structure on selectivity. *Applied Catalysis A: General*, 2002, **232**(1-2), 147-58.

2. Wagner, J.; Autenrieth, T. & Hempelmann, R. Core shell particles consisting of cobalt ferrite and silica as model ferrofluids $[CoFe_2O_4 - SiO_2]$ core shell particles. *J. Magnetism Magnetic Mater.*, 2002, **252,** 4-6.

3. Sun, S.; Murray, C.B.; Weller, D.; Folks, L. & Moser, A. Monodiserse *FePt* nanoparticles and ferromagnetic *FePt* Nanocrystal supperlattices. *Science*, 2000, **287**(5460), 1989-992.

4. Wu, M.; Zhang, Y.D.; Hui, S.; Xiao, T.D.; Ge, S.; Hines, W.A. & Budnick, J. I. Microwave magnetic properties of $Co_{50}/(SiO_2)_{50}$ nanoparticles. *Appl. Phys. Lett.*, 2002, **80**(23), 4404-406.

5. Kobayashi, T.; Haruta, M.; Sano, H. & Delmon, B. Optical detection of *CO* in air through catalytic chromism of metal-oxide thin films. *In* Proceedings of the Third International Meeting on Chemical Sensors, Cleveland, Ohio, USA, 1990. pp.318-21.

6. Maruyama, T. & Arai, S. Electrochromic properties of cobalt oxide thin films prepared by chemical vapour deposition. *J. Electrochem. Soc.*, 1996, **143**(4), 1383-386.

7. Švegl, F.; Orel, B.; Hutchinson, M.G. & Kalcher, K. Structural and spectroelectrochemical investigations of sol-gel derived electrochromic spinel Co_3O_4 films. *J. Electrochem. Soc.*, 1996, **143**(5), 1532-539.

8. Shinde, V.R.; Mahadik, S.B.; Gujar, T.P. & Lokhande, C.D. Supercapacitive cobalt oxide (Co_3O_4) thin films by spray pyrolysis. *Appl. Surf. Sci.*,2006, **252**(20), 7487-492.

9. Estrada, W.; Fantini, M.C.A.; Castro, S.C.D.; Fonseca, C.N.P.D. and Gorenstein, A. Radio frequency sputtered cobalt oxide coating: structural, optical, and electro-chemical characterisation. *J. Appl. Phys.*,1993, **74**(9), 5835-841.

10. Dasilva, L.M.; Boodts, J.F.C. & Faria, L.A.D. Oxygen evolution at $RuO_2(x) + Co_3O_4(1–x)$ electrodes from acid solution. *Electrochimica Acta*, 2001, **46**(9), 1369-375.

11. Jiang, S.P. & Tseung, A.C.C. Homogeneous and heterogeneous catalytic in cobalt oxide / graphite air electrodes. *J. Electrochem. Soc.*, 1990, **137**(3), 764-69.

12. Ni, Y.; Ge, X.; Zhang, Z.; Liu, H.; Zho, Z. & Ye, Q. A simple reduction-oxidation route to prepare Co_3O_4 nanocrystals. *Mater. Res. Bull.*, 2001, **36**, 2383-387.

13. Mousavand, T.; Takami, S.; Umetsu, M.; Ohara, S. & Adschiri, T. Supercritical hydrothermal synthesis of organic-inorganic hybrid nanoparticles. *J. Mater. Sci.*, 2006, **41**(5), 1445-448.

14. Vidal-Vidal, J.; Rivas, J. & López-Quintel, M.A. Synthesis of monodisperse maghemite nanoparticles by the microemulsion method. *Colloids and Surfaces A: Physicochem. Engg. Aspects*, 2006, **288**(1-3), 44-51.

15. Švegl, F.; Orel, B.; Svegl, I.G. & Kaucic, C.V. Characterisation of spinel Co_3O_4 and *Li*-doped Co_3O_4 thin film electrocatalysts prepared by the sol-gel route. *Electrochimica Acta*, 2000, **45**(25-26), 4359-371.

16. Takeshi, T.; Hamagamia, T.; Kawamurab, T.; Yamaki, J. & Tsuji, M. Laser ablation of cobalt and cobalt oxides in liquids: influence of solvent on composition of prepared nanoparticles. *Appl. Surf. Sci.*, 2005, **243**(1-4), 214-19.

17. Yuan, Z.; Huang F., Feng, C.; Sun, J. & Zhou, Y. Synthesis and electrochemical performance of nanosized Co_3O_4. *Mater. Chem. Phys.*, 2004, **79**(1),1-4.

18. Yang, H.; Hu, Y.; Zhang, X. & Qiu, G. Mechanochemical synthesis of cobalt oxide nanoparticles. *Materials Letters,* 2004, **58**(3-4), 387-89.

19. Sufi, R.A. & Kofinas, P. Magnetic properties and mor-phology of block copolymer cobalt oxide nanocomposites. *J. Magnetism Magnetic Mater.*, 2005, **288**, 219-23.

20. Athawale, A.A.; Bhagwat, S.V.; Katre, P.P.; Chandwadkar, A.J. & Karandikar, P. Aniline as a stabiliser for metal nanoparticles. *Materials Letters*, 2003, **57**(24-25), 3889-894.

21. Luis, P.; Xiomara, C.; Rodrý´guez, J.; Nieves, I.; Arce, R.; Garc´ýa, C. & Oyol, R. Spectroscopic and electrochemical properties of 2-aminophenothiazine. *J. Photochem. Photobio. A: Chemistry*, 2008, **198**(1), 85-91.

22. Zhang, H.; Wu, J.; Zhai, C.; Ma, X.; Du, N.; Tu, J. & Yang, D. From cobalt nitrate carbonate hydroxide hydrate nanowires to porous Co_3O_4 nanorods for high performance lithium-ion battery electrodes. *Nanotechnology*, 2008, **19**(3), 035711-715.

23. Zhu, Y.; Li, H.; Kolypin, Y. & Gedanken, A. Preaparation pf nanosized cobalt hydroxides and oxyhydroxide assisted by sonication. *J. Mater. Chem.,* 2002, **12**, 729-33.

24. Hong, B.; Shandong, L.; Jiang, X.; Du, Y. & Yang, C. Magnetic anisotropy in carbon encapsulated *Co/CoO* "lines" with large exchange bias. *Physics Letters A*, 2003, **307**(1), 69-75.

25. Hideyuki, Y. Protein-assisted nanoparticle synthesis. *Colloids and Surfaces A: Physicochem. Engg. Aspects*, 2006, **282–283**, 464-70.

26. Rong, M.Z.; Zhang, M.Q.; Wang, H.B. & Zeng, H.M. Surface modification of magnetic metal nanoparticles through irradiation graft polymerisation. *Appl. Surf. Sci.*, 2002, **200**(1-4), 76-93.

27. Kshirsagar, V.S.; Vijayanand, S.; Potdar, H.S.; Joy, P.A.; Patil, K.R. & Rode, C. V. Highly active nanostructured Co_3O_4 catalyst with tunable selectivity for liquid phase air oxidation of *p*-cresol. *Chemical Letters*, 2008, **37**(3), 310-11.

Contributors

Dr (Mrs) Anjali A. Athawale is Assoc Prof in the Department of Chemistry, University of Pune, Pune. She has been actively involved in research working on conducting polymers, metal nanoparticles, oxide–polymer nanocomposites and their applications as sensors as well as catalysts. She has published over 65 papers in international journals and has contributed a chapter in Encyclopedia of Sensors.

Dr Megha Majumdar had obtained her PhD in Chemistry from the University of Pune in 2008. She is currently pursuing her postdoctoral research at Tata Institute of Fundamental Research, Mumbai in Materials Chemistry. Her primary research interests are: Nanomaterials, metal and metal oxides, their synthesis, characterisation, and applications in catalysis.

Ms Hema Singh obtained her MSc in Applied Chemistry. Her areas of research are: Synthesis of oxide nanoparticles by various techniques and their use as materials for sensor applications.

Mr K. Navinkiran has done MSc in Materials science. Presently, he is pursuing PhD in the field of synthesis of nano sized oxides. His areas of interest include: Synthesis and characterisation of conducting polymers and oxides for catalysis applications.